Computational Investigation of Isoeugenol Transformations on a Platinum Cluster – I: Direct Deoxygenation to Propylcyclohexane

Francesco Ferrante[a,*], Chiara Nania[a], Dario Duca[a]

[a] *Dipartimento di Fisica e Chimica "E. Segrè" - Università degli Studi di Palermo, Viale delle Scienze Ed. 17, I-90128 Palermo, Italy*

Abstract

The growing demand for renewable and sustainable fuels, protagonists of an increasingly important research area due to the exhaustion of fossil resources, has oriented our investigation towards the computational mechanistic analysis of the catalytic hydrodeoxygenation (HDO) reaction of isoeugenol. Having the most common functional groups, the isoeugenol molecule is actually considered as an experimental and computational model for typical species of biomass origin. The reported computational investigation outlines the energy barriers and the intermediates along the path for the conversion of isoeugenol to propylcyclohexane through a direct deoxygenation mechanims, catalyzed by a subnanometric metal cluster. For this purpose, the Pt_{10} platinum cluster was chosen as the catalyst model, being this noble metal a reference for hydrogenation reaction. The results obtained rule the formation of the 4-propylphenol intermediate as the rate determining step for the considered branch of the mechanim, and as the pivotal point for further ramifications. The present is the first of a series of studies aimed to a complete mapping of isoeugenol HDO on a Pt cluster, to be used as reference for further, more focused, investigations, such as those regarding the effects of the support and of the metal particle size, as well as the HDO reaction of biomass-derived compounds similar to isoeugenol.

*Corresponding author

Email addresses: francesco.ferrante@unipa.it (Francesco Ferrante), chiara.nania@unipa.it (Chiara Nania), dario.duca@unipa.it (Dario Duca)

Keywords: DFT, Catalytic Reactions Mechanisms, Bio-oils, Biomass

1. Introduction

Pyrolysis of biomass gives rise to the formation of bio-oils, complex mixtures of compounds derived from the rapid and simultaneous depolymerization of cellulose, hemicellulose and lignin, following a rapid increase in temperature. Bio-oils are composed mainly by hydroxyaldehydes, hydroxyketones, sugars, carboxylic acids and phenols [1]. Hydrodeoxygenation reaction (HDO) of lignin-derived bio-oils is currently an important research area due to the depletion of fossil fuel resources, and is devoted to satisfy the increasingly pressing demand for renewable and sustainable alternatives for the production of fuels, chemicals and energy. Bio-oils as such are not suitable as fuels due to their acidity and high oxygen content, as well as their instability [2, 3]. Being a mixture of oxygenated components, they do not have the physico-chemical properties to compete, as a transport fuel, with petroleum distillates. However, their liquid form facilitates further processing, making the refining and upgrading of biofuel into liquid hydrocarbons an important process [4]. Various catalytic pathways for hydrogenation and deoxygenation of bio-oils have been extensively studied, but among these HDO is considered the most effective method [5]. Although there are some studies on the HDO of bio-oils, in order to facilitate the elucidation of the HDO reaction mechanism, it is preferred to replace more complex species with simpler models, consisting of monomeric lignin compounds. Due to its molecular structure, which contains the most common functional groups in bio-oils derived from lignin (i.e. hydroxyl, methoxy and allyl groups), isoeugenol can be considered as an appropriate and representative molecular candidate model.

Understanding catalytic processes at the atomic level is a fundamental goal of chemistry, and catalysis on supported metal cluster (SMC) systems play a role that is becoming more and more important in the modern chemical industry [6]. Indeed, following the recent developments of the synthetic methods aimed

at obtaining small metal cluster systems, the related catalysis approaches have rapidly become a subfield of heterogeneous catalysis and much effort is at present dedicated to the creation of specifically tailored SMC catalysts showing high efficiency and selectivity [7–11]. Stabilized on solid supports, such as metal oxides, silica, various forms of carbon, zeolites, and others [12–15] SMC are promising catalytic systems both for academic and industrial applications, being either able to catalyze reactions otherwise difficult to occur or to be separated quite easily at the end of the process [16].

Besides that, SMCs possess high surface/volume ratio, another very important feature is the presence of metal-to-metal bonds, that is, of nearby metal sites that offer greater possibilities for binding with the substrate [17]. Since many important catalytic processes require tightly cooperating metal sites for reactant adsorption, activation and product desorption, SMCs can be used in a wide variety of catalytic reactions [16, 18, 19]. SMCs, moreover, can show a certain structural fluidity during the catalytic process. At high temperatures and under the influence of metal-support and/or metal-substrate interactions, SMCs can actually lose their initial stiffness and evolve into fluxional species, generating metastable geometries that can increase reactivity [20]. The properties of metal clusters can also be selectively modified by introducing dopant atoms, which change their electronic structure, their relationship with the support and their catalytic activity as well [21].

Intensive research in recent years has shown that clusters size has a very large impact on their reactivity, as well as on the efficiency and selectivity of the catalytic processes in which they are involved [22]. There is a scalable regime, in which reactivity changes constantly with cluster size, and a non-scalable size regime for small clusters, in which reactivity could completely change even after adding a single atom [23]. This size-reactivity relationship can be explained in terms of the change in surface morphologies. Advances in this area have benefited from the development of accurate quantum-mechanical calculations, which became an increasingly powerful tools for understanding the processes that rule the structure of the catalyst and, ultimately, its catalytic performance.

It has been suggested [24–26] that HDO reaction of phenolics may occur with two limiting mechanisms depending on nature of the metal catalyst: deoxygenation-through-hydrogenation, HYD, according to which the first steps involved concern the hydrogenation of the benzene ring, and direct deoxygenation mechanism, DDO, meaning that the saturation of benzene ring occurs after removal of oxigen-containing groups. The present work is the first of a series aimed to elucidating, by means of an atomistic approach based on density functional theory, the whole mechanism of HDO of phenolics on noble and non-noble subnanometric metal clusters, in order to reveal how the reduced size of the catalyst may affect the outcomes of the reaction. Here the HDO reaction of isoeugenol catalyzed by a small platinum cluster is presented. Isoeugenol and platinum are, in fact, considered as models for compounds of biomass origin and for hydrogenation catalyst [27, 28], respectively. Among the many foreseeable pathways, it was decided to follow the DDO mechanims on a platinum cluster in order to create a reference for future investigations with other, possibly non-noble, catalytic systems and to find key points for possible branches of the mechanism which could lead to significant differences in catalytic activity and selectivity between noble and non-noble metals. Further, a reference mechanism reported for an unsupported cluster can be used to identify the effects that various kind of supports could have on important stages of the hydrodeoxygenation process.

After a short section concerning the preliminary study on H_2 fragmentation and H diffusion on the platinum cluster, the computational data collected on the elementary processes characterizing the surface species involved in the hydrogenation are reported and analyzed to detail one of the possible mechanisms for the reaction that converts isoeugenol into propylcyclohexane.

2. Computational Details and Models

All the calculations were performed in the framework of density functional theory (DFT), using the Gaussian 16 package [29]. The B3LYP hybrid exchange-

correlation functional [30] was used and the D3 correction scheme developed by Grimme (GD3), which allows one to take into account dispersion interactions [31], was added to the functional. For the conformational study of isoeugenol, the correlation consistent polarized valence double zeta (cc-pVDZ) basis set by Dunning and coworkers [32] was used. The study of isoeugenol HDO reaction on the platinum cluster was instead carried out with the LANL2DZ basis set [33, 34]; this, developed by Hay and Wadt, uses Dunning's basis set (D95) [35] for light atoms (H, C, O) and, for platinum, a double-zeta valence basis set associated to an effective core potential. Polarization functions consisting of primitive Gaussians having angular momentum and exponents in accordance with the following scheme have been added to the D95 set: H (s: 0.049, p: 0.587), C (p: 0.0311, d: 0.587), O (p: 0.0673, d: 0.961). These functions were retrieved from the EMSL Basis Set Exchange website [36]. Minima and transition state (TS) species on the reaction paths were revealed by inspection of the harmonic vibrational frequencies, checking that imaginary frequencies were not present in the structures corresponding to potential energy surface minima and only one imaginary frequency (corresponding to the one related to the eigenmode transforming reactant to the product) was present in the TS structures. In one case, due to the difficulty of finding the transition state for a whole molecule rearrangement (see Section 3.4), the nudged elastic band approach was used, as implemented in the Empathes code [37, 38].

The energetics of the reaction paths will be given in terms of vibrational zero-point corrected energies (E_{ZPV}); the desorption energies of intermediates and final product has been corrected for the basis set superposition error (BSSE) by using the counterpoise method of Boys and Bernardi [39]. Since BSSE was calculated as correction to the SCF energy, it will be reported in parenthesis along with the uncorrected E_{ZPV} energies.

A magic number [40] corresponding to a regular tetracapped octahedron [41] platinum cluster shaped by ten atoms, having T_d symmetry and spin multiplicity equal to 9, was chosen as the subnanometric catalytic model [42]. Its structure shows the presence of atoms with different coordination. The four

cap atoms have actually coordination three, while the remaining six atoms have coordination number six. These determine the octahedron cage, on whose triangular faces the cap atoms are arranged. In particular, two platinum cap atoms with coordination three are found in the upper portion of the octahedron, while the other two in the lower portion, arranged on a plane perpendicular to that where the first two lie. The geometry of Pt_{10} cluster is represented in Figure 1, along with the numbering used throughout for the carbon atom centers in the isoeugenol molecule and all its derivatives up to propylbenzene.

[Figure 1 about here.]

3. Results and discussion

The simultaneous presence, in the isoeugenol molecule, of some of the most common functional groups characteristic of bio-oils opens up several possibilities for the HDO reaction study. In this first work, the HDO mechanism on a platinum cluster was investigated according to the four consecutive stages

1. saturation of allyl double bond;
2. removal of metoxy group;
3. removal of hydroxy group;
4. saturation of benzene ring.

which, apart from the first process, represent a typical DDO mechanism. This follows one of the experimental hypotheses put forth by the research group of D.-Yu. Murzin, which, in the aim to employ low cost catalysts, conducted their experiments using nickel [2, 43]. The computational results obtained will be reported in the next sections, starting from the preliminary investigation on the H_2 fragmentation and H diffusion on the Pt_{10} cluster and the interaction of isoeugenol with the catalytic system.

3.1. Fragmentation of H_2 on Pt_{10}

As evidenced by other studies [42], the Pt_{10} cluster has nonect spin multiplicity and tetrahedral geometry. The Pt−Pt bond lengths in the optimized

structure are in the range 2.60-2.82 Å, with an average value of 2.71 Å. The longest linear dimension of the cluster is therefore slightly less than 6 Å. The binding energy of the cluster with respect to ten isolated Pt atoms in the d^9s^1 electronic configuration is equal to 2754.0 kJ mol^{-1}; therefore the cohesive energy, calculated as $E_c = (E[Pt_{10}] - 10E[Pt])/10$, is equal to 275.4 kJ mol^{-1}.

It has been already claimed that H_2 molecule, once chemisorbed on a given metal cluster, undergoes bond cleavage leading to the formation of hydrogen-species/metal-cluster systems in which the hydrogen atoms diffuse freely. In this case, the model catalyst, therefore, can be considered as a reservoir of hydrogen, ensuring a continuous availability of H atoms where necessary. This because, in addition to the ease of hydrogen fragmentation on the cluster, free diffusion of the hydrogen atoms through the catalyst could be hypothesized. To corroborate these inferences, demonstrated for most of metal systems [44, 45], fragmentation and diffusion tests were carried out considering one H_2 molecule on the Pt_{10} cluster, in the following represented as $Pt_{10}H_2$ species.

As far as fragmentation is concerned, the chemisorption of the H_2 molecule on the platinum cap atom, showing coordination three, was considered. Adsorption, characterized by an energy release equal to 80.5 kJ mol^{-1}, led to the formation of a transient species with multiplicity of spin 9 (Figure 2a), in which a considerable weakening of the $H \cdots H$ bond (length of 0.88 Å against 0.74 Å in the free H_2 molecule) is observed. The latter rapidly evolves into a species of 32.5 kJ mol^{-1} more stable (Figure 2b), in a septet spin multiplicity state, that undergoes transformation by cluster distortion, paralleled by the total fragmentation of H_2. In this species, it has been found that the migration of a hydrogen atom from the top position on a cap site to a bridge arrangement involving the same cap atom and one neighboring atom belonging to the octahedron cage (Figure 2c) has an activation barrier equal to 6.8 kJ mol^{-1}, i.e. an almost negligible low energy value.

[Figure 2 about here.]

For the diffusion process, the geometries of five $Pt_{10}2\,H$ arrangements, char-

acterized by different hydrogen constellations were considered. A further verification in support of the easy diffusion of the hydrogen atoms through the cluster was performed by considering the two most stable species, indicated in Figure 3 with the letters (a) and (c), and the process of H atom migration converting one into the other. The estimated activation barrier of this elementary event, equal to 14.3 kJ mol^{-1}, clearly demonstrates the validity of the assumptions made above.

[Figure 3 about here.]

In view of these results, it can be stated that in the conditions needed to overcome the activation barriers occurring in the isoeugenol HDO, which will be discussed later, the barriers characterizing the hydrogen atom diffusion on the $Pt_{10}2\,H$ fragments are negligible. This implies that the hydrogen atoms can be arranged in any configuration on the cluster. It is finally to be underlined that, as it happens in the case of a large number of metal clusters [44, 46, 47], the fragmentation of H_2 is the cause of the decrease of one unit of the spin quantum number observed in the $Pt_{10}2\,H$ systems, being this occurrence correlated to electron spin coupling phenomena.

3.2. Adsorption of isoeugenol on $Pt_{10}2\,H$

There are six conformations for the *trans* isomer of isoeugenol, three of which are obtained by keeping the dihedral angle τ_1(C5C4C1′C2′) fixed at 180° and fixing, alternatively, the value of the τ_2(C2C1OH) and τ_3(C1C2OC1″) angles to 0° and 180°; the other three conformations can be obtained by keeping the dihedral angle τ_1 fixed at 0° and imposing, alternatively, the values 0° and 180° for the τ_2 and τ_3 angles. An equal number of conformations obvioulsy exist for the *cis* isomer. In it, however, the dihedral angle τ_1 has been set to 150°, because of the steric repulsion between the CH_3 group of the allyl chain (outside the plane identified by the aromatic ring) and the hydrogen atom of the C3 of the ring.

The twelve starting structures thus generated were subjected to geometry optimization. Not surprisingly, the most stable conformations for both stereoisomers are those where an intramolecular hydrogen bond occurs between the hydroxyl hydrogen and the metoxy oxygen, *i.e.* $\tau_2 = 180°$ and $\tau_3 = 0°$. In these conformations there is flexibililty as regard the rotation of the allyl chain, resulting in Boltzmann populations of 62.8% ($\tau_1 = 180°$) and 37.1% ($\tau_1 = 0°$) for the *trans* isomer, and of 55.2% ($\tau_1 = 152°$) and 44.8% ($\tau_1 = -33°$) for the *cis* isomer. The *trans* stereoisomer of isoeugenol was calculated to be ca. 10 kJ mol^{-1} more stable than the *cis* one.

The adsorption of the most stable conformation of *trans*-isoeugenol on the lowest energy configuration of $Pt_{10}2\,H$ was therefore investigated. The various tests performed to find the adsorption geometry of isoeugenol on the cluster allowed to conclude that, in the most stable structure, the compound interacts with a cap platinum by means of the carbon atoms, C1′ and C2′, of the allyl chain as well as through the benzene ring with the lower portion of a cluster edge, involving a site of the octahedron cage. The adsorption of isoeugenol does not affect the spin multiplicity of the system, which remains in the septet state, but causes the two H atoms to shift from top to edge positions in the cluster, likely due to electron donation from the benzene ring to the metal centers [48]: the H−Pt bond length increases (from 1.54 to 1.64 Å) and the H atoms do interact also with another metal center (at distance equal to 1.82 Å), thus stabilizing configurations like the one showed in Figure 3(b). The adsorption energy of isoeugenol is equal to -237.7 (BSSE = 28.3) kJ mol^{-1}. This value, which is quite high if one looks at adsorption studies of simple alkenes on metal clusters [49], is indeed justified by the presence of the aromatic component which strongly interacts with the cluster. By calculating, with the same computational methods, the adsorption energy of propene on $Pt_{10}2\,H$, it was possible to roughly estimate that the energetic contribution of the aromatic portion to the adsorption of isoeugenol is about 140 kJ mol^{-1}, thus representing more than half of the total interaction energy.

In the optimized *trans*-isoeugenol/$Pt_{10}2\,H$ system a hydrogen atom is neigh-

boring to the site where the first catalytic hydrogenation could take place, corresponding to the saturation of the allyl chain.

3.3. Hydrogenation of allyl group

The elementary steps involved in the catalytic hydrogenation of the isoeugenol double bond on the Pt_{10} cluster are reported in Figure 4. The process is formed by two elementary steps: the first one leads to the formation of a semi-hydrogenated intermediate, int1/$Pt_{10}H^a$, by transferring the H atom from the cluster to the C2′ carbon atom of the allyl group; in the second one the migration of one H atom from the cluster to the C1′ atom of the chain with the formation of dihydroeugenol/Pt_{10} is conversely involved. In this and in all the other cases discussed below, the letter δ inside a circle indicates the diffusion of a hydrogen atom through the cluster towards the reactive center; here the already supposed barrier-free H-diffusion transforms int1/$Pt_{10}H^a$ into int1/$Pt_{10}H^b$. On the basis of the activation energies of the two elementary steps, it can be noticed that the hydrogenation of the double bond should not be a fast process: energies barriers are indeed slightly higher than those calculated for the reaction converting butene to butane on a subnanometric palladium cluster [45].

The double bond saturation leads to a system, which is 106.3 kJ mol^{-1} less stable than the isoeugenol/Pt_{10}2 H reactant. This is not unexpected, since the dihydroeugenol interacts with the metal cluster only by means of the benzene ring. The desorption energy of dihydroeugenol from the cluster is calculated as 154.7 (BSSE = 25.7) kJ mol^{-1}.

[Figure 4 about here.]

3.4. Formation of 4-propylphenol

The next stage of the reaction should be the removal of the OCH_3 group from the adsorbed dihydroeugenol and the subsequent formation of 4-propylphenol. To investigate this reaction, two major channels can be hypotesized: i) the direct cleavage of the methoxy group, with the final formation of methanol and 4-propylphenol, or ii) the cleavage of the methyl group, giving rise to methane,

water and 4-propylphenol as products and a cathecol derivative as intermediate. One or two hydrogen molecules are needed for the first and second case, respectively. It has been reported that the route involving the production of methane is the one actually preferred when platinum or even non noble metals are used as catalysts for the HDO reaction of phenolics [50–52]; nonetheless, since details of cluster catalysis still have to be discovered, both the hypotesized mechanisms were taken into consideration hence investigated.

Following the methanol channel it must be considered that, according to preliminary calculations, the H atom residing on the platinum cluster is not able to protonate the oxygen atom of the methoxy group, meaning that this mechanism should involve the breaking of the C2−O bond with the migration of the OCH_3 fragment toward a platinum atom (that, as a consequence, become hexacoordinated in an octahedral environment), its protonation and subsequent desorption. In order to trigger the C−O bond breaking it was necessary to rearrange the dihydroeugenol adsorbed on the cluster; in Figure 5 and in the following a structural rearrangement is indicated by the symbol ρ inside a circle. The new form of dihydroeugenol/Pt_{10} is ca. 25 kJ mol^{-1} less stable than the one produced by the allyl group saturation, but it shows the methoxy group correctly aligned with a platinum cluster edge. In order to verify the ease with which this rearrangement takes place, the minimum energy path connecting the two adsorption geometries of dihydroeugenol on the cluster was searched by using a nudged elastic band approach. The maximum along the path revealed an energy barrier of 34 kJ mol^{-1}, a value suggesting a good mobility of the adsorbed species. The rearrangement of dihydroeugenol prompts the shift of the OCH_3 moiety toward the cluster, with an energy barrier of 107.1 kJ mol^{-1}. It is interesting to note that in the resulting (int2+CH_3O)/Pt_{10} intermediate, the hydrogen bond, already observed in the most stable conformations of isoeugenol and dihydroeugenol and taking place between the hydroxyl H and the methoxy O centers, does not break. On the contrary, it is shortened from 2.13 to 1.63 Å. This allows the formation of methanol to occur almost instantly by H-shift from the hydroxyl group, without the intervention of catalyst acti-

vated hydrogen. Finally, a stabilizing H-bond (with length 1.47 Å) is present in the (int3+CH_3OH)/Pt_{10} product. As usual, this highlights a sharing of the H atom between the two oxygen atoms connected. The phenomen, presumably originated by the limited size of the Pt_{10} cluster and connected to its relatively high flexibility, was not taken into account before by experimental hypotheses, related to HDO reactions involving either isoeugenol or related compounds [53, 54]. This remark deserves to be underlined since implicitly emphasizes how catalytic processes on subnanometric clusters do not always follow the established rules of heterogeneous catalysis and conversely do represent a case by case chemistry to be investigated.

[Figure 5 about here.]

In order to proceed with the HDO reaction, the methanol molecule was desorbed from the cluster (desorption energy equal to 100.7 kJ mol^{-1}, with BSSE = 11.6 kJ mol^{-1}) and a new H_2 molecule was fragmented on it; the int3/Pt_{10}2 H system so originated was used as starting point for the formation of an adsorbed 4-propylphenol species. In the optimized geometry, the int3 species interacts through the dangling O atom and the C2 of the benzene ring with the upper portion of one edge of the cluster, including one cap and one octahedron cage atom; therefore the aromatic portion, placed almost perpendicular to the cluster, does not interact significantly with it except for the single carbon atom indicated above. The migration of a H atom from the cluster to the oxygen atom of int3 (see Figure 6) leads to the int4/$Pt_{10}H^a$ intermediate, which, after hydrogen diffusion, forms int4/$Pt_{10}H^b$. In the second elementary step, 4-propylphenol/Pt_{10} is finally formed. The interaction energy of this compound with the platinum cluster is 159.2 (BSSE = 9.3) kJ mol^{-1}.

[Figure 6 about here.]

The first elementary step of the reaction highlights that the hydrogenation of the oxygen atom is not a simple process because various factors, connected to each other, concur to the stabilization of the reacting system. Oxygen and,

in particular, the radical C2 carbon atom give rise to strong bonds with platinum that have to be weakened for hydrogenation to take place. In fact, the energy barrier (171.6 kJ mol^{-1}) for this elementary event would be the highest of the whole process. This indeed seems to be the point in which significant bifurcations of the mechanism could occur: the hydrogen atom could migrate from the cluster towards the oxygen or the carbon atom. In the second case, the reduction of the benzene ring would be triggered, with oxygen maintaining the interaction of the fragment with the cluster. The hydrogenation of oxygen could take place subsequently, with the formation of 4-propylcyclohexanol. The investigation of this mechanism, along with possible parasite reactions and undesired products, will be the subject of future investigations.

In the present work, the purpose of which, as already said, is to detail the "direct" deoxygenation of isoeugenol, it was considered that the formation of the int4 intermediate could actually occur before the desorption of CH_3OH. Indeed, the hydrogen bond in (int3+CH_3OH)/Pt_{10} could maintain the position of the dangling oxygen atom, inhibiting its interaction with platinum and making it available for hydrogenation. This is actually the case, since as can be seen from Figure 7, the energy barrier to trasform (int3+CH_3OH)/Pt_{10}2 H to (int4+CH_3OH)/Pt_{10}H is 129.6 kJ mol^{-1}, i.e. more than 40 kJ mol^{-1} lower than that occurring in the int3/Pt_{10}2 H to int4/Pt_{10}H conversion. Moreover, the hydrogenation of the oxygen atom in (int3+CH_3OH)/Pt_{10}2 H occurs with an energy release of 57 kJ mol^{-1}, to be compared to the 10.3 kJ mol^{-1} of energy required for the same process in the absence of coadsorbed methanol. Since the hydrogen bond is weakened, methanol could desorb more easily from (int4+CH_3OH)/Pt_{10}H (desorption energy of 76.1 kJ mol^{-1}, with BSSE equal to 9.7 kJ mol^{-1}), giving rise to int4/$Pt_{10}H^a$ (after a rearrangement releasing 7 kJ mol^{-1} of energy), which in turn can be hydrogenated to 4-propylphenol following the same path already depicted in Figure 6. It is worth to note that the energy barrier for the first hydrogenation step sensibly decreases, due to the presence of coadsorbed methanol, but it still shows the highest barrier that was found along the DDO mechanism.

[Figure 7 about here.]

Let's now take into consideration the second channel for the formation of 4-propylphenol, the one resulting in the production of methane. Starting again from adsorbed and rearranged dihydroeugenol on Pt_{10}, the $O-CH_3$ bond breaking involves a energy barrier of 123.4 mol^{-1} (Figure 8a), which is slightly higher than the one calculated for the methoxy group cleavage and gives a int2′ intermediate coadsorbed with a methyl group. When two H atoms are inserted in the system, the methyl group, located atop a three-coordinated Pt atom, is easily hydrogenated to methane (Figure 8b), which in turn easily desorbs. The int2′ intermediate and one hydrogen atom are therefore left on the metal cluster; H-diffusion could let the two species react to form the O−H bond of a cathecol derivative, the 4-propylbenzene-1,2-diol, whose desorption would require 133.9 kJ mol^{-1} (BSSE = 27.1 kJ mol^{-1}) of energy. As reported in Figure 8c, the cleavage of the OH group from this intermediate occur by overcoming an energy barrier of 114.1 mol^{-1}, which is roughly the same as the one for the methoxy counterpart. The road to 4-propylphenol continues in Figure 9, after that two further hydrogen atoms were added: water is promptly formed and, following H diffusion, the int3′ intermediate is saturated to the phenol derivative.

[Figure 8 about here.]

[Figure 9 about here.]

Based on the energy barriers involved, it can be concluded that the two reaction paths leading from dihydroeugenol to 4-propylphenol on the Pt_{10} cluster can be considered essentialy competitive. However it must be taken into account that one more hydrogen molecule is consumed in the methane path, where the formation of $CH_4 + H_2O$ instead of CH_3OH occurs.

3.5. Formation of propylbenzene

The hydroxyl elimination process from 4-propylphenol consists of two elementary steps: the first involves the cleavage of the C1−O bond and the adsorption of the OH fragment on one face of the cluster; the second step is the

hydrogenation of the OH and the desorption of a water molecule from the cluster. The reaction profile reported in Figure 10a shows that the breaking of the C−O bond, with an energy barrier of 115.6 kJ mol^{-1}, is almost as easy as the hydrogenation reaction of the double bond, and that it leads to the formation of a slightly more stable system, here labelled as (int5+OH)Pt_{10}. On the other hand, from Figure 10b it is evident that the passage of the H atom from the cluster to the OH is an easy process, being its energy barrier equal to 73.3 kJ mol^{-1}. The water molecule thus formed has a calculated desorption energy equal to 97.2 (BSSE = 18.9) kJ mol^{-1}. The last elementary process (Figure 10c), showing an energy barrier of 92.7 kJ mol^{-1}, is the transfer of one H atom from the cluster to the phenyl C atom, which leads to the formation of the stable propylbenzene. The desorption energy of this species from the cluster is 152.9 (BSSE = 30.3) kJ mol^{-1}.

[Figure 10 about here.]

3.6. Total reduction of propylbenzene to propylcyclohexane

The reduction of the aromatic ring has attracted renewed attention in the chemical and petroleum industries, thanks to its application in the synthesis of a variety of useful chemical intermediates [55]. However, from an experimental point of view the development of highly efficient hydrogenation processes under mild and, hopefully, solvent-free conditions is still a challenge. From the computational side, however, a number of studies have made it possible to obtain a detailed description of the hydrogenation mechanism of benzene; the results have shown that it likely follows a Horiuti-Polanyi scheme [56], which involves the consecutive addition of hydrogen adatoms. Although there is a modest literature on benzene hydrogenation, nothing seems to be reported for propylbenzene; it can be easily argued, however, that its reduction to propylcyclohexane could occur through simple successive additions of hydrogen atoms, similarly to the benzene case. As a matter of fact, this mechanism must, in fact, be adapted to the specific hydrogenation process of phenyl, belonging to

the propylbenzene adsorbed on Pt_{10}. This presents some difficulties, associated with various factors, the most evident of which is the impossibility of being able to discriminate, *a priori*, the most reactive carbon atoms of the ring on the basis of the electronic effects of the substituent (propyl chain). Furthermore, the addition of hydrogen, which can be defined as a "ghost" atom due to its size, does not allow one to confidently exploit the information that could be acquired by considering things in terms of steric hindrance. Therefore, not having firm theoretical or practical support, it was necessary to proceed with consecutive hydrogenations, taking into consideration every single carbon atom of the ring as a potential reactive site.

The results of our analysis regarding the total hydrogenation of propylbenzene on Pt_{10} are collected schematically in Scheme 1. In reading this scheme it must be noted that (i) the H atoms of propylbenzene are not showed; (ii) the circled numbers near a figure refer to the position of benzene ring where catalytic hydrogen will attach; (iii) yellow circles represent carbon site directly interacting with the platinum atoms of the cluster; (iv) on the right of each figure the energy barrier and the energy of the product (relative to the reactant of the corresponding elementary step, the former, and to the starting reactant, the latter) are reported, separated by a semicolon; (v) two new H atoms are inserted in the system when needed for consecutive hydrogenations; (vi) the energetics of what is considered the kinetically and thermodinamically preferred hydrogenation path is reported inside a box and the corresponding structure is the reactant of the subsequent elementary step.

[Scheme 1 about here.]

On the basis of the considerations above, for the first catalytic hydrogenation the passage of one H atom from the cluster to four chemically different C atoms of the propylbenzene ring was investigated, i.e. the carbon bearing the propyl group and the carbon atoms in *ortho-*, *meta-* and *para-* position to it. Therefore, four elementary steps were considered, and for each of them the structures of reagent, product and transition state were calculated. The results

obtained show that the passage of the H atom from the cluster to the C of the ring occurs preferentially in position 2. This elementary step is favored, with respect to the other three, both at the kinetic and thermodynamic level since its activation barrier is equal to 94.3 kJ mol^{-1} and the intermediate obtained is the most stable. Then we proceeded, starting from intermediate **I**, with the second elementary step. In order to identify the second most reactive site, the hydrogenation of the residual unsaturated carbon atoms of the ring was investigated one at a time. It can be observed that the second elementary hydrogenation, for the same reasons as the previous one, takes place preferentially on C1. It has an energy barrier of 41.8 kJ mol^{-1}, much lower than the others obtained and it leads to the most stable product. It can be noted that the first catalytic hydrogenation on propylbenzene occurs in a similar way to hydrogenation of a double bond. It leads to the formation of a stable species, the 5-propyl-1,3-cyclohexadiene (**II**), whose desorption energy is 244.6 (BSSE = 26.2) kJ mol^{-1}.

The first elementary step of the second catalytic hydrogenation involved all the unsaturated carbon atoms of **II**. For each hypothetical reactive site, similarly to what was done previously, the reagent, product and transition state were estimated and optimized. The reaction scheme for the second catalytic hydrogenation highlights that the transfer of the first H atom preferentially takes place on the carbon in position 4. The resulting intermediate **III**, in which the electron density is delocalized on the remaining three carbon atoms of the ring, shows a thermodynamic stability similar to that found for the intermediate obtained by attaching one H atom in position 3; for the latter, however, there is a much higher energy barrier to overcome.

Starting from the semi-hydrogenated intermediate **III**, the passage of the second H atom from the cluster to carbon atoms 1, 2 and 3 of the ring, respectively, was investigated. The energies of the products and the energy barriers for each stage, however, do not allow us to discriminate which of the three elementary steps should occur preferentially, in either kinetic or thermodynamic terms. For this reason, the carbon atoms in position 1, 2 and 3 were con-

sidered equally reactive sites and, therefore, it was considered appropriate to continue with the third catalytic hydrogenation on each of them. This leads to the competing formation of two stable products, 3-propylcyclohexene **IV** and 4-propylcyclohexene **VI**, which can desorb from the cluster with 196.8 (BSSE = 9.3) and 173.6 (BSSE = 26.3) kJ mol^{-1}, respectively. On the other hand, the intermediate **V**, which due to its diradicalic character has a stability comparable to that of **IV** and **VI**, evidently due to favorable interactions with platinum, cannot desorb from the cluster.

The first step of the third catalytic hydrogenation, involving 3-propylcyclohexene **IV**, shows that the transfer of the atom H from the cluster occurs preferentially on the C2 site of the ring. The activation barrier of path 2 is much lower than that of the alternative path; this allows us to indicate this as the favored path not only on a kinetic level, because the corresponding barrier is the lowest, but also from a thermodynamic point of view. The semi-hydrogenated intermediate **VII**, in fact, is more stable, by 17.1 kJ mol^{-1}, than the equivalent intermediate derived from path 1. The second H atom was therefore added on the last unsaturated carbon atom of intermediate **VII**, thus leading to the formation of propylcyclohexane **VIII** in the chair conformation. Its desorption energy from the cluster is 140.4 (BSSE = 19.6) kJ mol^{-1}.

The first elementary step of the third catalytic hydrogenation, involving intermediate **V** shows that the semi-hydrogenated intermediate **IX**, not only should form more rapidly because it has an activation barrier of about 24.7 kJ mol^{-1} lower than that pinpointed along the formation of the semi-hydrogenated intermediate resulting from the other path but it is also the most thermodynamically stable. Therefore, it was considered just the transfer of the second hydrogen atom on this intermediate. In this way propylcyclohexane **X** was obtained in a distorted boat conformation, the second more stable form of cyclohexane (desorption energy equal to 130.7 kJ mol^{-1} with BSSE = 22.4 kJ mol^{-1}).

Finally, as regards 4-propylcyclohexene **VI**, the preferred first elementary step of the third catalytic hydrogenation has an energy barrier of 55.9 kJ mol^{-1}

and gives the intermediate **XI**, even if it must be noticed that the species resulting from the other path is certainly more stable. The hydrogenation of **XI** create a distorted boat conformation of propylcyclohexane **XII**, whose desorption energy from the cluster is 108.1 (BSSE = 21.0) kJ mol^{-1}. Incidentally, at the level of theory used in this work, the chair and distorted boat conformations of propylcyclohexane differ by 25 kJ mol^{-1}, a value in agreement with the 21 kJ mol^{-1} reported in the literature for cyclohexane [57].

4. Conclusions and Future Directions

The present investigation, which is part of a more ambitious project, does not aim at rigorously compare theoretical and experimental data but to elucidate the HDO reaction mechanism on a standard metal, namely platinum, cluster (Pt_{10}) in order to identify the elementary steps and intermediate reaction routes, hence to outline the possible ramifications and parallel processes of greatest interst.

The investigated sequence of steps for isoeugenol HDO was the one experimental hypotesized for non-noble catalysts, according to which the first molecular fragment that undergoes catalytic hydrogenation is the double bond on the allyl chain, leading to dihydroeugenol, then the reaction proceeds through a direct deoxygenation mechanism. According to the reported results based on DFT calculations, the removal of the OCH_3 moiety following the route leading to the formation of methanol (which resulted essentially competitive to the one producing methane and water) would not take place by simple transfer of one hydrogen atom from the cluster to the methoxy group, but by cleavage of the C−O bond and subsequent hydrogenation of the chemisorbed fragment by the hydroxy group of the same substrate molecule. This would generate an intermediate where a dangling oxygen atom is stabilized by a very strong hydrogen bond with the coadsorbed methanol. If atomic hydrogen is available at this stage on the cluster, the hydrogenation of the intermediate above would first restore the hydroxyl group and subsequently form 4-propylphenol. On the contrary, if methanol desorbs before the hydrogenation of the dangling oxygen atom occurs,

the intermediate would rearrange on the cluster to give a geometry where the interactions with the cluster would hamper the formation of 4-propylphenol, due to a very high energy barrier along the path. This point of the mechanism seems therefore to be crucial for the whole HDO to propylcyclohexane and could constitute one of the step where the most significant bifurcations of the mechanism occur. Once formed, 4-propylphenol loses the OH group by cleavage of the C−OH bond and the subsequent hydrogenation of the fragment, which desorbs as water. When the aromaticity of the system is restored by transferring one hydrogen atom from the cluster to the unsaturated carbon, propylbenzene is formed. This, after three consecutive catalytic hydrogenations, leads finally to propylcyclohexane, in its distorted boat conformation. The whole process producing propylcyclohexane starting from isoeugenol:

$$C_{10}H_{12}O_2 + 6H_2 \rightarrow C_9H_{18} + CH_3OH + H_2O$$

is finally characterized by a calculated Gibbs free energy difference equal to -309.6 kJ mol^{-1}.

The present work can be considered as the starting point to investigate the possible different reaction paths characterizing HDO reactions on different metal clusters, in order to provide experimental chemists with useful tools (such as the identification of the largest number of secondary and/or parasitic products) for the optimization of the process conducted on a large scale.

Future perspectives are precisely i) investigating the HYD channel for isoeugenol conversion to propylcyclohexane, ii) investigating reaction paths potentially involved that lead to other products, such as propylcyclohexanol or benzene and cyclohexene derivatives originating by disproportionation of cyclohexadiene derivatives, as well as iii) conducting the same reaction using non-noble and inexpensive metal catalysts, such as nickel, in order to determine their activity and selectivity with respect to those shown by the platinum clusters.

Acknowledgements

The authors would like to thank professor Dmitry Yu. Murzin at Åbo Akademi University of Turku (Fin) for having truly inspired us by this topic and for the fruitful discussions.

References

[1] D. Mohan, C. U. Pittman, P. H. Steele, Pyrolysis of wood-biomass for bio-oil: a critical review, Energy & Fuels 20 (2006) 848–889. doi:10.1021/ef0502397.

[2] S. Tieuli, P. Mäki-Arvela, M. Peurla, K. Eränen, J. Wärnà, G. Cruciani, F. Menegazzo, D. Y. Murzin, M. Signoretto, Hydrodeoxygenation of isoeugenol over Ni-SBA-15: kinetics and modelling, Appl. Cat. A: Gen. 580 (2019) 1–10. doi:10.1016/j.apcata.2019.04.028.

[3] P. Mäki-Arvela, D. Murzin, Hydrodeoxygenation of lignin-derived phenols: from fundamental studies towards industrial applications, Catalysts 7 (2017) 265. doi:10.3390/catal7090265.

[4] D. C. Elliott, Transportation fuels from biomass via fast pyrolysis and hydroprocessing, in: Advances in Bioenergy, John Wiley & Sons, Ltd, 2016, pp. 65–72. doi:10.1002/9781118957844.ch6.

[5] J. Feng, C.-Y. Hse, Z. Yang, K. Wang, J. Jiang, J. Xu, Liquid phase in situ hydrodeoxygenation of biomass-derived phenolic compounds to hydrocarbons over bifunctional catalysts, Appl. Cat. A: General 542 (2017) 163–173. doi:10.1016/j.apcata.2017.05.022.

[6] U. Heiz, E. L. Bullock, Fundamental aspects of catalysis on supported metal clusters, J. Mater. Chem. 14 (2004) 564–577. doi:10.1039/B313560H.

[7] G. Ertl, H.-J. Freund, Catalysis and surface science, Physics Today 52 (2008) 32. doi:10.1063/1.882569.

[8] G. A. Somorjai, The flexible surface: new techniques for molecular level studies of time dependent changes in metal surface structure and adsorbate structure during catalytic reactions, J. Mol. Cat. A: Chem. 107 (1996) 39–53. doi:10.1016/1381-1169(95)00227-8.

[9] F. Arena, F. Ferrante, R. Di Chio, G. Bonura, F. Frusteri, L. Frusteri, A. Prestianni, S. Morandi, G. Martra, D. Duca, DFT and kinetic evidences of the preferential CO oxidation pattern of manganese dioxide catalysts in hydrogen stream (PROX), Appl. Catal. B: Env. 300 (2022) 120715. doi:10.1016/j.apcatb.2021.120715.

[10] L. Gueci, F. Ferrante, A. Prestianni, F. Arena, D. Duca, Benzyl alcohol to benzaldehyde oxidation on MnO_x clusters: Un- raveling atomistic features, Mol. Catal. 513 (2021) 111735. doi:10.1016/j.mcat.2021.111735.

[11] L. Gueci, F. Ferrante, A. Prestianni, R. D. Chio, T. Patti, D. Duca, F. Arena, DFT insights into the oxygen-assisted selective oxidation of benzyl alcohol on manganese dioxide catalysts, Inorg. Chim. Acta 511 (2020) 119812. doi:10.1016/j.ica.2020.119812.

[12] A. Prestianni, R. Cortese, F. Ferrante, R. Schimmenti, D. Duca, S. Hermans, D.-Y. Murzin, α-d-glucopyranose adsorption on a Pd_{30} cluster supported on boron nitride nanotube, Top. Catal. 59 (2016) 1178–1184. doi:10.1007/s11244-016-0638-3.

[13] F. Ferrante, A. Prestianni, R. Cortese, R. Schimmenti, D. Duca, Density functional theory investigation on the nucleation of homo- and heteronuclear metal clusters on defective graphene, J. Phys. Chem. C 120 (2016) 12022–12031. doi:10.1021/acs.jpcc.6b02833.

[14] R. Schimmenti, R. Cortese, F. Ferrante, A. Prestianni, D. Duca, Growth of sub-nanometric palladium clusters on boron nitride nanotubes: A DFT study, Phys. Chem. Chem. Phys. 18 (2016) 17450–1757. doi:10.1039/C5CP06625E.

[15] A. Prestianni, F. Ferrante, E. M. Sulman, D. Duca, Density functional theory investigation on the nucleation and growth of small palladium clusters on a hyper-cross-linked poly-styrene matrix, J. Phys. Chem. C 118 (2014) 21006–21013. doi:10.1021/jp506320z.

[16] C. Dong, Y. Li, D. Cheng, M. Zhang, J. Liu, Y.-G. Wang, D. Xiao, D. Ma, Supported metal clusters: fabrication and application in heterogeneous catalysis, ACS Catalysis 10 (2020) 11011–11045. doi:10.1021/acscatal.0c02818.

[17] B. J. Holliday, Surface and interfacial organometallic chemistry and catalysis. Topics in organometallic chemistry, J. Am. Chem. Soc. 129 (2007) 3772–3773. doi:10.1021/ja0697065.

[18] K. Koichumanova, A. K. K. Vikla, R. Cortese, F. Ferrante, K. Seshan, D. Duca, L. Lefferts, In situ atr-ir studies in aqueous phase reforming of hydroxyacetone on Pt/ZrO_2 and Pt/AlO(OH) catalysts: The role of aldol condensation, Appl. Catal. B: Env. 232 (2018) 454–463. doi:10.1016/j.apcatb.2018.03.090.

[19] R. Cortese, R. Schimmenti, F. Ferrante, A. Prestianni, D. Decarolis, D. Duca, Graph-based analysis of ethylene glycol decomposition on a palladium cluster, J. Phys. Chem. C 121 (2017) 13606–13616. doi:10.1021/acs.jpcc.7b00850.

[20] H. Zhai, A. N. Alexandrova, Fluxionality of catalytic clusters: when it matters and how to address it, ACS Catalysis 7 (2017) 1905–1911. doi:10.1021/acscatal.6b03243.

[21] H. Häkkinen, S. Abbet, A. Sanchez, U. Heiz, U. Landman, Structural, electronic, and impurity-doping effects in nanoscale chemistry: supported gold nanoclusters, Angew. Chemie Int. Ed. Eng. 42 (2003) 1297–1300. doi:10.1002/anie.200390334.

[22] S. M. Lang, T. M. Bernhardt, Gas phase metal cluster model systems for heterogeneous catalysis, Phys. Chem. Chem. Phys. 14 (2012) 9255–9269. doi:10.1039/C2CP40660H.

[23] O. Hübner, H.-J. Himmel, Metal cluster models for heterogeneous catalysis: a matrix-isolation perspective, Chem. Eur. J. 24 (2018) 8941–8961. doi:10.1002/chem.201706097.

[24] M. Hellinger, H. W. P. Carvalho, S. Baier, D. Wang, W. Kleist, J. D. Grunwaldt, Catalytic hydrodeoxygenation of guaiacol over platinum supported on metal oxides and zeolites, Appl. Catal. A: Gen. 490 (2015) 181–192. doi:10.1016/j.apcata.2014.10.043.

[25] H. Lee, H. Kim, M. J. Yu, C. H. Ko, J. K. Jeon, J. Jae, S. H. Park, S. C. Jung, Y. K. Park, Catalytic hydrodeoxygenation of bio-oil model compounds over Pt/HY catalyst, Sci. Rep. 6 (2016) 28765. doi:10.1038/srep28765.

[26] A. Bielić, M. Grilc, B. Likozar, Catalytic hydrogenation and hydrodeoxygenation of lignin-derived model compound eugenol over Ru/C: Intrinsic microkinetics and transport phenomena, Chem. Eng. J. 333 (2018) 240–2659. doi:10.1016/j.cej.2017.09.135.

[27] D. Duca, F. Frusteri, A. Parmaliana, G. Deganello, Selective hydrogenation of acetylene in ethylene feedstocks on Pd catalysts, Appl.Catal. A: Gen. 146 (1996) 269–284. doi:10.1016/S0926-860X(96)00145-7.

[28] R. Schimmenti, R. Cortese, L. Godina, A. Prestianni, F. Ferrante, D. Duca, D. Y. Murzin, A combined theoretical and experimental approach for platinum catalyzed 1,2-propanediol aqueous phase reforming, J. Phys. Chem. C 121 (2017) 14636–14648. doi:10.1021/acs.jpcc.7b03716.

[29] M. J. Frisch, G. W. Trucks, H. B. Schlegel, G. E. Scuseria, M. A. Robb, J. R. Cheeseman, G. Scalmani, V. Barone, G. A. Petersson, H. Nakatsuji, X. Li, M. Caricato, A. V. Marenich, J. Bloino, B. G. Janesko, R. Gomperts,

B. Mennucci, H. P. Hratchian, J. V. Ortiz, A. F. Izmaylov, J. L. Sonnenberg, D. Williams-Young, F. Ding, F. Lipparini, F. Egidi, J. Goings, B. Peng, A. Petrone, T. Henderson, D. Ranasinghe, V. G. Zakrzewski, J. Gao, N. Rega, G. Zheng, W. Liang, M. Hada, M. Ehara, K. Toyota, R. Fukuda, J. Hasegawa, M. Ishida, T. Nakajima, Y. Honda, O. Kitao, H. Nakai, T. Vreven, K. Throssell, J. A. Montgomery, Jr., J. E. Peralta, F. Ogliaro, M. J. Bearpark, J. J. Heyd, E. N. Brothers, K. N. Kudin, V. N. Staroverov, T. A. Keith, R. Kobayashi, J. Normand, K. Raghavachari, A. P. Rendell, J. C. Burant, S. S. Iyengar, J. Tomasi, M. Cossi, J. M. Millam, M. Klene, C. Adamo, R. Cammi, J. W. Ochterski, R. L. Martin, K. Morokuma, O. Farkas, J. B. Foresman, D. J. Fox, Gaussian 16 Revision C.01 (2016).

[30] A. D. Becke, A new mixing of Hartree–Fock and local density-functional theories, J. Chem. Phys. 98 (1993) 1372–1377. doi:10.1063/1.464304.

[31] S. Grimme, J. Antony, S. Ehrlich, H. Krieg, A consistent and accurate ab initio parametrization of density functional dispersion correction (DFT-D) for the 94 elements H-Pu, J. Chem. Phys. 132 (2010) 154104. doi:10.1063/1.3382344.

[32] T. H. Dunning, Gaussian basis sets for use in correlated molecular calculations. I. The atoms boron through neon and hydrogen, J. Chem. Phys. 90 (1989) 1007–1023. doi:10.1063/1.456153.

[33] P. J. Hay, W. R. Wadt, Ab initio effective core potentials for molecular calculations. potentials for K to Au including the outermost core orbitals, J. Chem. Phys. 82 (1985) 299–310. doi:10.1063/1.448975.

[34] P. J. Hay, W. R. Wadt, Ab initio effective core potentials for molecular calculations. Potentials for the transition metal atoms Sc to Hg, J. Chem. Phys. 82 (1985) 270–283. doi:10.1063/1.448799.

[35] T. H. Dunning, P. J. Hay, Gaussian Basis Sets for Molecular Calculations,

in: H. F. Schaefer (Ed.), Methods of Electronic Structure Theory, Modern Theoretical Chemistry, Springer US, 1977, pp. 1–27.

[36] B. P. Pritchard, D. Altarawy, B. Didier, T. D. Gibson, T. L. Windus, New basis set exchange: an open, up-to-date resource for the molecular sciences community, J. Chem. Inf. Model. 59 (2019) 4814–4820. doi:10.1021/acs.jcim.9b00725.

[37] M. Bertini, F. Ferrante, D. Duca, Empathes: A general code for nudged elastic band transition states search, Comp. Phys. Commun. 271 (2022) 108224. doi:10.1016/j.cpc.2021.108224.

[38] Climbing-image nudged elastic band was employed with 10 images along the reaction path and a threshold of 0.003 Hartree bohr^{-1} on the forces.

[39] S. F. Boys, F. Bernardi, The calculation of small molecular interactions by the differences of separate total energies. Some procedures with reduced errors, Mol. Phys. 19 (1970) 553–566. doi:10.1080/00268977000101561.

[40] M. Brack, Metal clusters and magic numbers, Scientific American 277 (1997) 50–55, publisher: Scientific American, a division of Nature America, Inc.

[41] R. B. King, Applications of Graph Theory and Topology in Inorganic Cluster and Coordination Chemistry, CRC Press, 1992, Ch. 6.4.E, p. 94.

[42] I. Demiroglu, K. Yao, H. A. Hussein, R. L. Johnston, DFT global optimization of gas-phase subnanometer Ru–Pt clusters, J. Phys. Chem. C 121 (2017) 10773–10780. doi:10.1021/acs.jpcc.6b11329.

[43] C. Lindfors, P. Mäki-Arvela, P. Paturi, A. Aho, K. Eränen, J. Hemming, M. Peurla, D. Kubička, I. L. Simakova, D. Y. Murzin, Hydrodeoxygenation of isoeugenol over Ni- and Co-supported catalysts, ACS Sustain. Chem. Eng. 7 (2019) 14545–14560. doi:10.1021/acssuschemeng.9b02108.

[44] F. Ferrante, A. Prestianni, M. Bertini, D. Duca, H_2 transformations on graphene supported palladium cluster: DFT-MD simulations and NEB calculations, Catalysts 10 (2020) 1306. doi:10.3390/catal10111306.

[45] V. D'Anna, D. Duca, F. Ferrante, G. La Manna, DFT studies on catalytic properties of isolated and carbon nanotube supported Pd_9 cluster : Part II. hydro-isomerization of butene isomers, Phys. Chem. Chem. Phys. 12 (2010) 1323–30. doi:10.1039/b920949m.

[46] V. D'Anna, D. Duca, F. Ferrante, G. L. Manna, DFT studies on catalytic properties of isolated and carbon nanotube supported Pd_9 cluster - I: Adsorption, fragmentation and diffusion of hydrogen, Phys. Chem. Chem. Phys. 11 (2009) 4077–4083. doi:10.1039/b820707k.

[47] G. Barone, D. Duca, F. Ferrante, G. L. Manna, CASSCF/CASPT2 analysis of the fragmentation of H_2 on a Pd_4 cluster, Int. J. Quant. Chem. 110 (2010) 558–562. doi:10.1002/qua.22119.

[48] M. T. de M. Cruz, J. W. de M. Carneiro, D. A. G. Aranda, M. Bühl, Density functional theory study of benzene adsorption on small Pd and Pt clusters, J. Phys. Chem. C 111 (2007) 11068–11076. doi:https://doi.org/10.1021/jp072572c.

[49] F. Mittendorfer, C. Thomazeau, P. Raybaud, H. Toulhoat, Adsorption of unsaturated hydrocarbons on Pd(111) and Pt(111): A DFT study, J. Phys. Chem. B 107 (2003) 12287–12295. doi:10.1021/jp035660f.

[50] R. Shu, R. Li, B. Lin, C. Wang, Z. Cheng, Y. Chen, A review on the catalytic hydrodeoxygenation of lignin-derived phenolic compounds and the conversion of raw lignin to hydrocarbon liquid fuels, Biomass and Bioenergy 132 (2020) 105432. doi:https://doi.org/10.1016/j.biombioe.2019.105432.

[51] D. Gao, Y. Xiao, A. Varma, Guaiacol hydrodeoxygenation over platinum catalyst: Reaction pathways and kinetics., Ind. Eng. Chem. Res. 10638-10644 (2015) 54. doi:10.1021/acs.iecr.5b02940.

[52] T. Nimmanwudipong, C. Aydin, J. Lu, R. C. Runnebaum, K. C. Brodwater, N. D. Browning, D. E. Block, B. C. Gates, Selective hydrodeoxygenation of guaiacol catalyzed by platinum supported on magnesium oxide, Catal. Lett. 142 (2012) 1190–1196. doi:https://doi.org/10.1007/s10562-012-0884-3.

[53] M. Alda-Onggar, P. Mäki-Arvela, K. Eränen, A. Aho, J. Hemming, P. Paturi, M. Peurla, M. Lindblad, I. L. Simakova, D. Y. Murzin, Hydrodeoxygenation of isoeugenol over alumina-supported Ir, Pt, and Re catalysts, ACS Sustain. Chem. Eng. 6 (2018) 16205–16218. doi:10.1021/acssuschemeng.8b03035.

[54] L. Bomont, M. Alda-Onggar, V. Fedorov, A. Aho, J. Peltonen, K. Eränen, M. Peurla, N. Kumar, J. Wärna, V. Russo, P. Mäki-Arvela, H. Grénman, M. Lindblad, D. Y. Murzin, Production of cycloalkanes in hydrodeoxygenation of isoeugenol over Pt- and Ir-modified bifunctional catalysts, Eur. J. Inorg. Chem. 2018 (2018) 2841–2854. doi:10.1002/ejic.201800391.

[55] H. Liu, R. Fang, Z. Li, Y. Li, Solventless hydrogenation of benzene to cyclohexane over a heterogeneous Ru–Pt bimetallic catalyst, Chem. Eng. Sci. 122 (2015) 350–359. doi:10.1016/j.ces.2014.09.050.

[56] M. Saeys, M.-F. Reyniers, M. Neurock, G. B. Marin, Ab initio reaction path analysis of benzene hydrogenation to cyclohexane on Pt(111), J. Phys. Chem. B 109 (2005) 2064–2073. doi:10.1021/jp049421j.

[57] J. Clayden, N. Greeves, S. Warren, Organic Chemistry, OUP Oxford, 2012.

TOC entry

Computational Investigation of Isoeugenol Transformations on a Platinum Cluster – I: Direct Deoxygenation to Propylcyclohexane

Francesco Ferrante, Chiara Nania, Dario Duca

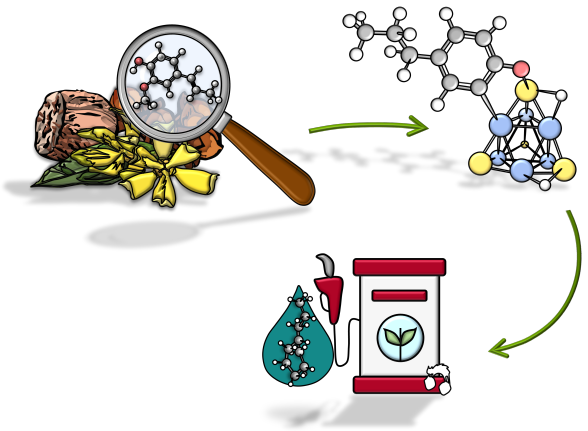

List of Figures

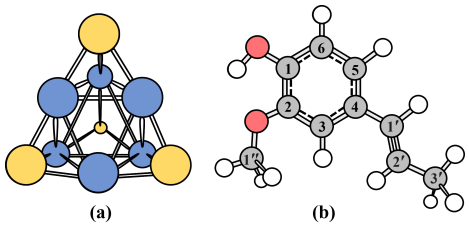

Figure 1: (a) Pt_{10} cluster, model of the subnanometric catalyst; the Pt atoms with different coordination numbers are distiguished by different colors (yellow and light blue for coordination number three and six, respectively). (b) Molecular structure of *trans*-isoeugenol with the IUPAC numbering of carbon atoms.

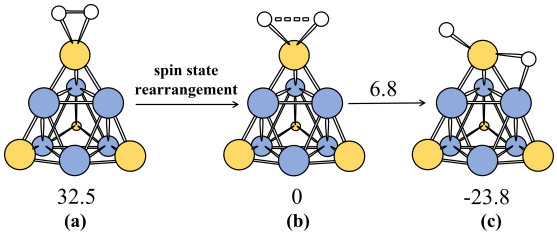

Figure 2: Fragmentation of the H_2 molecule on the Pt_{10} cluster and relative energies of the species involved (in kJ mol^{-1}). Structure (a) is a transient species in nonect state in which there is a weakening of the $H \cdots H$ bond, (b) is the most stable species, with septet spin multiplicity and (c) is the final structure (always a septet) in which the total fragmentation of the H_2 molecule occurs, through the migration of one hydrogen atom from its initial top position towards a bridge arrangement on the cluster. White, yellow and light blue balls identify hydrogen and platinum with coordination number three and six, respectively.

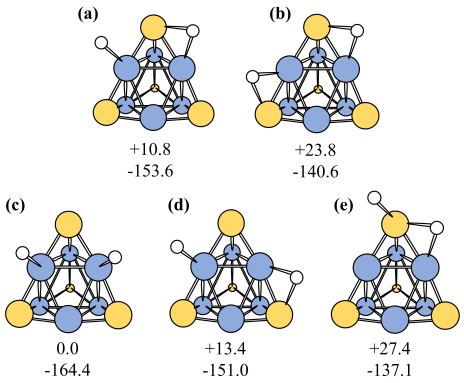

Figure 3: $Pt_{10}2\,H$ fragments: The five structures, labeled with the letters (a)-(e), differ from each other for the positions of the H atoms in the cluster; they were used to evaluate the H-diffusion energetics. The values below each figure indicate the relative energy (in kJ mol^{-1}) with respect to the most stable (c) configuration (up), and the H_2 chemisorption energy (down), calculated as E_{ads}=E[$Pt_{10}H_2$]-(E[Pt_{10}]+E[H_2]). White, yellow and light blue balls identify hydrogen and platinum with coordination number three and six, respectively.

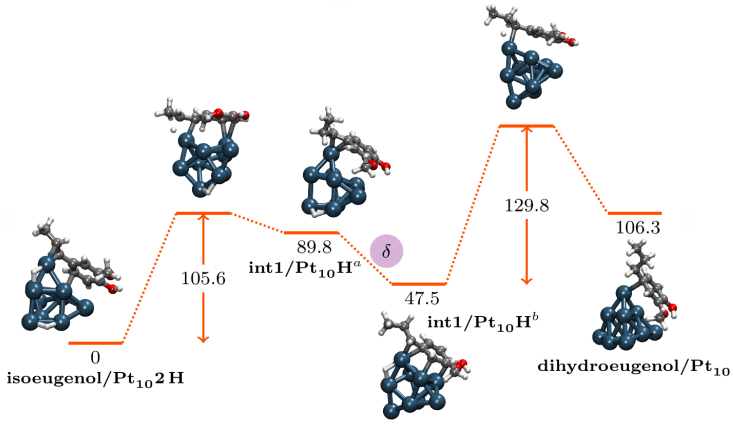

Figure 4: Reaction profile of the steps involved in the isoeugenol catalytic hydrogenation to dihydroeugenol on the Pt_{10} cluster. The δ symbol inside a circle indicates an elementary step characterized by an assumed barrier-less diffusion of the H atom across the cluster toward the catalytic site.

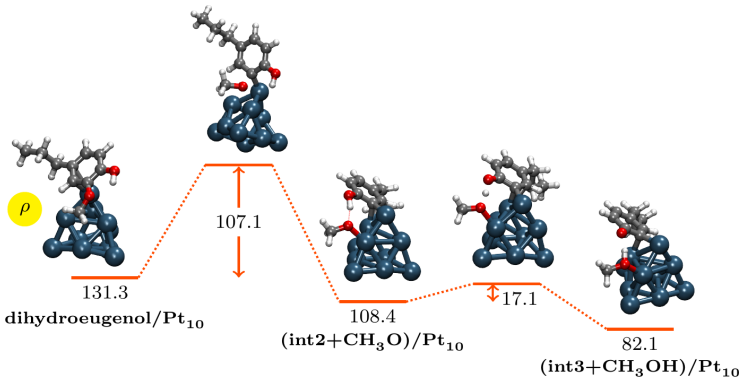

Figure 5: Reaction profile related to the C2−O bond cleavage and the subsequent formation of CH_3OH on the Pt_{10} cluster. The whole process takes place on the same potential energy surface of the first catalytic hydrogenation, implying that the energies of the intermediates refer to the isoeugenol/$Pt_{10}H_2$ system. The Greek letter ρ inside the circle indicates a structural rearrangement of dihydroeugenol on the cluster.

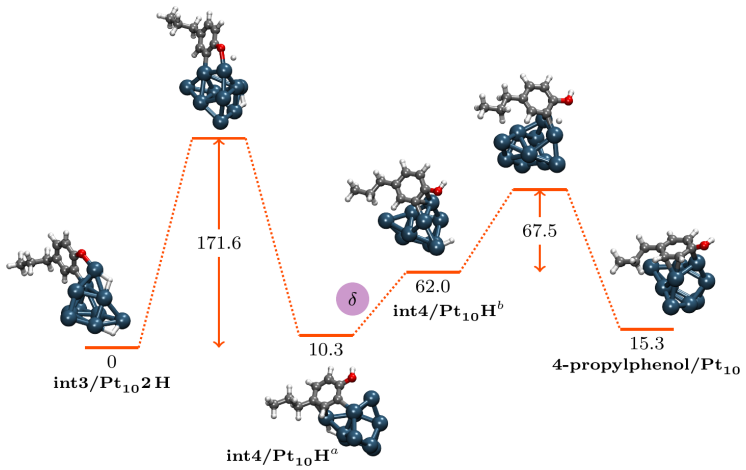

Figure 6: Reaction profile showing the restoration of the −OH fragment and the formation of the adsorbed 4-propylphenol species. Energies of the reaction intermediates refer to the catalytic hydrogenation system obtained following the desorption of methanol and the placement of two new H atoms on the cluster. The letter δ indicates the rapid diffusion of one H atom through the cluster.

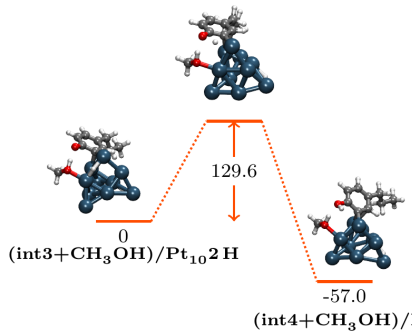

Figure 7: The direct formation of the int4 intermediate from (int3+CH_3OH)/Pt_{10}2 H occurring by an elementary step where two hydrogen atoms are inserted in the cluster before methanol desorbs.

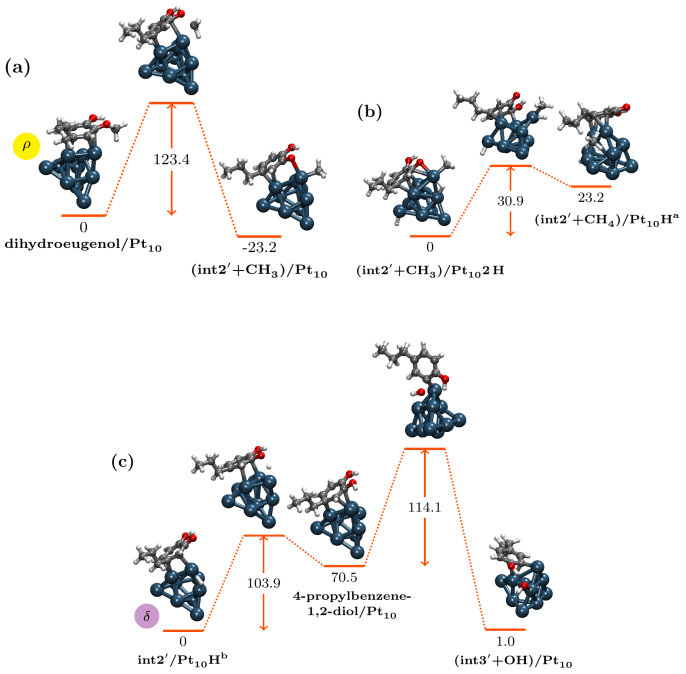

Figure 8: DFT calculated reaction profile related to the O−CH_3 bond cleavage (a) and the formation of CH_4 (b) on the Pt_{10} cluster. The C2−O bond breaking occurs after the formation of a cathecol derivative as intermediate (c).

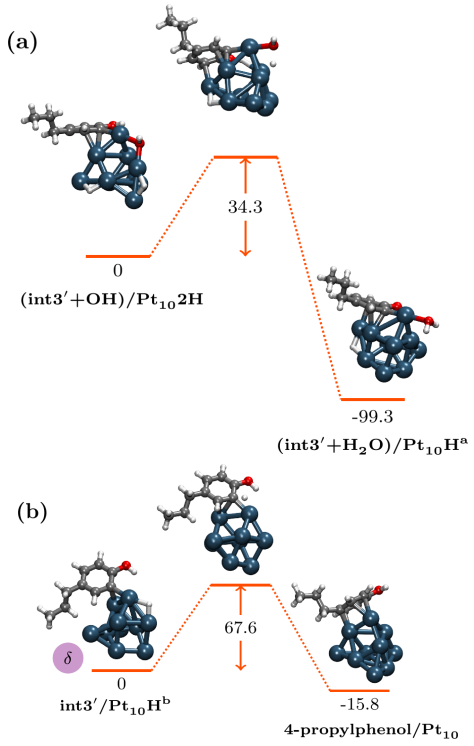

Figure 9: The easy formation of the water molecule (a) and the saturation of int3′ to 4-propylphenol in the methane channel.

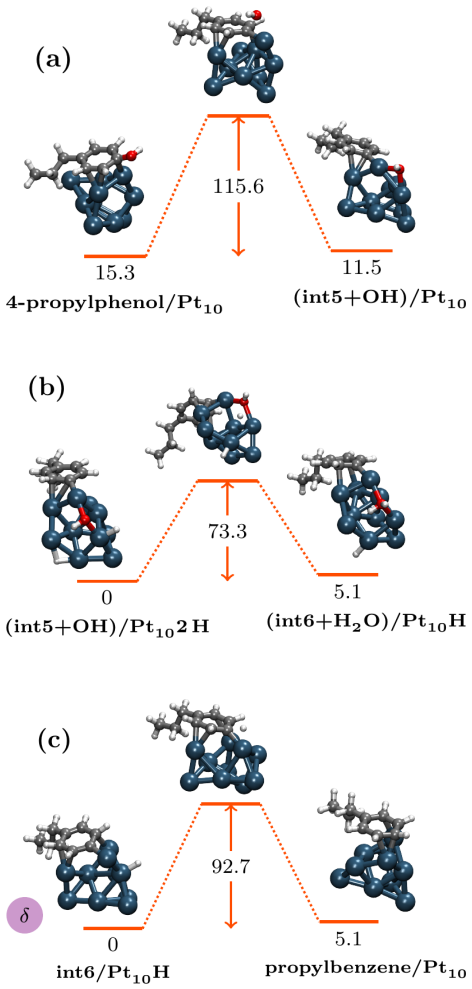

Figure 10: Reaction profiles related to (a) the cleavage of the C1−OH bond, (b) the hydrogenation of the OH fragment adsorbed on one face of the cluster and (c) the passage of a H atom from the cluster to C1. In (c) the highlighted δ indicates the diffusion, following the desorption of the H_2O molecule, of the H atom through the cluster.

List of Scheme

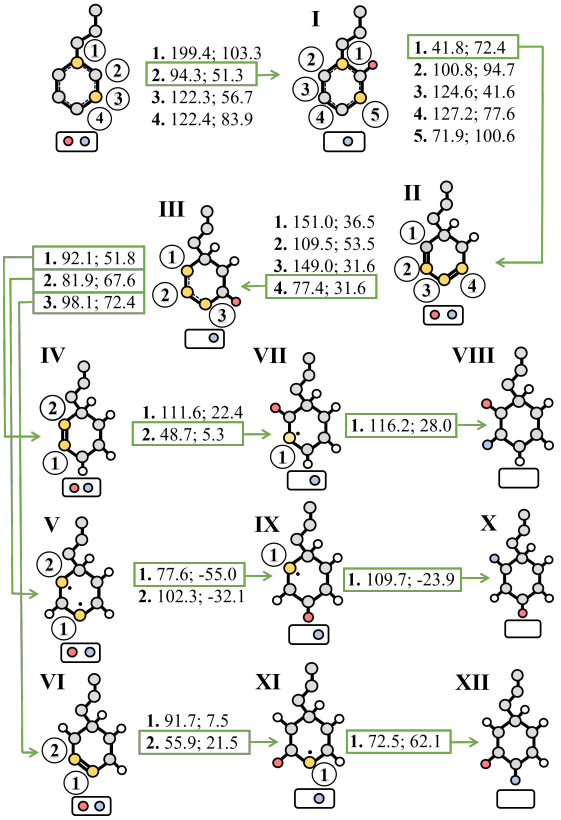

Scheme 1: Representation of the whole saturation of the benzene ring present in propylbenzene on the Pt_{10} cluster. The latter is represented by the small rectangle under the sketched molecular species; adsorbed hydrogen atoms are depicted as red and blue circles inside the rectangle, the not adsorbed ones are conversely not shown; yellow circles represent the interaction sites of the molecule with the cluster. In each entry, the first number is the position where catalytic hydrogen attaches, the second is the energy barrier of the corresponding elementary step, the third is the energy of the product, always referred to the reactant with two H atoms still on Pt_{10}. All energy values are expressed in kJ mol^{-1}. The first catalytic hydrogenation starts from propylbenzene, the second one from **II** (5-propyl-1,3-cyclohexadiene), the last one from **IV** (3-propylcyclohexene), **V** and **VI** (4-propylcyclohexene).